Applied Catalysis A: General 391 (2011) 297–304

Contents lists available at ScienceDirect

Applied Catalysis A: General

journal homepage: www.elsevier.com/locate/apcata

Bis(pyridyl)siloxane–Pd(II) complex catalyzed oxidation of alcohol to aldehyde: Effect of ligand tethering on catalytic activity and deactivation behavior

Michael N. Missaghi, John. M. Galloway, Harold H. Kung*

Department of Chemical and Biological Engineering, Northwestern University, Evanston, IL 60208, United States

ARTICLE INFO

Article history:
Received 27 February 2010
Received in revised form 3 August 2010
Accepted 16 September 2010
Available online 29 September 2010

Keywords:
Partial oxidation
Pd(II) catalysis
Ligand tethering
Pyridylsiloxane

ABSTRACT

A series of oligomeric methylsiloxane compounds functionalized with pyridyl groups was synthesized and used as ligands in the aerobic $Pd(OAc)_2$-catalyzed oxidation of benzyl alcohol to benzaldehyde at 353 K. The effect of tethering two pyridine ligands at the terminal positions of linear siloxanes of varying length was systematically investigated, as was the effect of the attachment point of the pyridine ring (*meta* or *para*). It was found that *meta*-substituted pyridylsiloxanes were generally more effective in protecting the catalyst against Pd agglomeration. For this purpose, the optimal *meta*-pyridylsiloxane ligands had 4–6 silicon atoms or 10 silicon atoms for *para*-pyridylsiloxane ligands. The metal–ligand binding properties were used to interpret the catalytic behavior, and the ability of the catalyst stability correlated with ability of the bis-pyridyl ligand to form a mononuclear cyclic complex with Pd.

1. Introduction

Palladium acetate $Pd(OAc)_2$-catalyzed aerobic oxidation of alcohols to carbonyl compounds, first reported in 1998, is an appealing method to replace environmentally unfriendly oxidants with molecular oxygen in processes of commercial importance [1]. Among the $Pd(OAc)_2$ systems studied, the $Pd(OAc)_2$/pyridine (*py*) catalyst system developed by Uemura and coworkers were found to be practical for preparative synthetic work [2]. The many derivative studies based on this catalyst system have been summarized in several reviews [3–5]. Of particular interest are approaches which enable the catalysis to proceed at room temperature and/or under 1 atm of air [6–8], and successful efforts to introduce enantioselectivity to the active site using a chiral ligand [6–8]. A common concern regarding these systems is the stability of the catalyst – in particular, the tendency of soluble Pd to aggregate into metallic nanoparticles with loss of activity.

Mechanistic studies on this catalyst system suggest that the alcohol oxidation takes place through a palladium alkoxide intermediate which reductively eliminates, along with two equivalents of AcOH, to give a $(py)_2Pd^0$ intermediate [9–10]. This zero-valent Pd species is readily attacked by O_2 to form either a peroxo or a hydroperoxide species which reacts with AcOH to regenerate the cationic Pd resting state, releasing H_2O_2 [11]. However, it could also form a Pd–Pd bond with another complex, release the *py* ligands, and form Pd agglomerates. Therefore, one approach to improve the stability of this catalyst is to protect the sensitive Pd^0 intermediate against agglomeration, while maintaining its reactivity towards O_2. Typically this can be done by using excess *py* ligand to shift the dissociation equilibrium towards the bound state. While effective, the presence of excess *py* substantially decreases the observed catalytic activity, and also necessitates the removal of the excess ligand from the reaction products.

Tethering two pyridyl ligands with a flexible spacer offers an alternative to the use of excess pyridine, since an increased local concentration of pyridyl species may stabilize the active Pd center without resorting to using excess ligands. In addition, such ligands can be designed to tune the active site environment by adjusting the length and flexibility of the tether. While a variety of oligomeric spacers are available for this purpose, we have investigated linear methylsiloxanes in this work due to the unique conformational properties of the Si–O–Si linkage. In particular, we suppose that the highly flexible Si–O backbone can accommodate the rigid and sterically demanding *trans* square planar geometry of coordination complexes of Pd^{II} [12].

We investigated the dependence of the catalytic properties on the separation distance between the pyridyl groups in the ligands, the attachment point of Si to the pyridine ring, the Pd concentration, the ligand–metal ratio, and the substrate–catalyst ratio. The results of our investigation are reported here.

2. Experimental

2.1. Ligands

Scheme 1 shows the ligands used and their designation. Details of the preparation and purification of the bis-(*meta*-

* Corresponding author.
E-mail address: hkung@northwestern.edu (H.H. Kung).

0926-860X/$ – see front matter © 2010 Elsevier B.V. All rights reserved.
doi:10.1016/j.apcata.2010.09.008

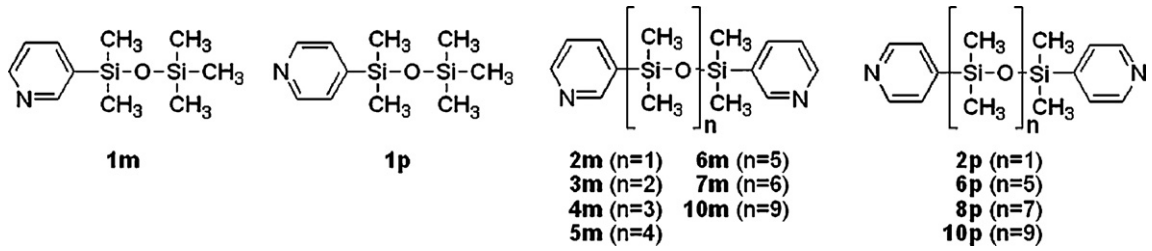

Scheme 1. Structures of pyridylsiloxane ($^s py$) ligands studied in this work.

pyridyl)siloxane ligands have been reported [13]. Those for the bis-(*para*-pyridyl)siloxane ligands can be found in the Appendix. They are low- to medium-viscosity oils at room temperature, and were found by ^{1}H NMR and elemental analysis to be free of detectable impurities. In order to distinguish siloxane-substituted pyridines from unsubstituted pyridine *py*, the former will be labeled $^s py$. In this paper, the ligand–metal ratios *py*:Pd or $^s py$:Pd were calculated on the basis of total pyridyl groups, noting that each bis(pyridyl)siloxane ligand contributes two pyridyl groups.

2.2. Catalysis experiments

Catalytic reactions were carried out in the batch mode in the liquid phase at 353 K under an atmospheric pressure of O_2. Freshly prepared (<1 week old) stock solutions of 25 mM $Pd(OAc)_2$ (Aldrich, 99.9% grade) in toluene, stored in the dark, was used as the Pd source. Stock solutions of benzyl alcohol (BnOH) in toluene (0.250, 1.00, and 4.00 M), stored in tightly closed vials, and stock solutions of ligand (0.8 N of $^s py$ in toluene) were also prepared. The latter was prepared by weighing the mass of ligand and assuming a ligand density of 1 g/mL.

The reactors were 4 mL glass vials, each equipped with a septum and a 10 mm × 3 mm PTFE-coated magnetic stirring bar. The vials were placed in tightly fit wells in an aluminum block which was heated by a temperature-controlled hotplate. Typically, 12 experiments were conducted simultaneously in 12 different vials, and a thermocouple was placed in the thirteenth vial, charged with the same volume of solvent and a stirring bar, for temperature control. The oxygen atmosphere (~7 kPa gauge pressure) above the liquid in the vials was maintained by an oxygen distributor, constructed with 12 Luer-Lok needle connection ports and 21-gauge 1.5 in. needles that punctured through the septa.

In a typical experiment, the reaction vials were charged with the required volumes of $Pd(OAc)_2$ solution, toluene solvent, and ligand solution to achieve the desired system concentration and ligand–metal ratio. For example, to achieve a 2:$^s py$–metal ratio and a final Pd concentration of 5 mM, 0.40 mL of 25 mM $Pd(OAc)_2$ solution (0.010 mmol), 0.025 mL of 0.8 N ligand solution (0.020 mmol $^s py$ ligand), and 1.37 mL of toluene would be added by pipette. The vials were placed in the Al block, tightly closed, vented with short 23-gauge needles, and connected to the oxygen distributor. An oxygen atmosphere was established by bubbling O_2 at room temperature for 10–15 min while the solution was stirred (400 rpm unless otherwise noted), after which the vent needles were removed and the oxygen supply needles were raised above the liquid level to prevent siphoning, but remained inserted into the vial to resupply O_2 consumed during reaction. The reaction block was heated to 353 ± 0.5 K. After the temperature reading was stabilized, the catalytic reaction was commenced by injecting 0.2–0.4 mL of 0.25–4.0 M BnOH in toluene into the vials. At regular intervals, a 0.1 mL sample was withdrawn by a syringe and diluted with 0.7 mL of $CDCl_3$ in a standard 5 mm NMR tube. The combination of dilution and cooling to room temperature effectively quenched the catalytic reaction. At the end of the experiment, the reaction vials were removed from the heating block and examined visually for coloration or darkening associated with Pd black formation. In the majority of cases, the reaction mixture was clear and colorless to light yellow after reaction; exceptions are noted in the text.

2.3. Determination of effect of stirring rate on reaction rates

The potential effect of O_2 dissolution on reaction kinetics was examined by investigating the effect of stirring rate using a reaction mixture containing 0.1 M BnOH, 5 mM $Pd(OAc)_2$, and pyridine (*py*:Pd = 2) at 353 K. Pyridine was used since its complexes were the most active. It was found that doubling the stirring rate from 400 to 800 rpm increased the reaction rate at short reaction times (2–6 min) by less than 5%. However, halving the stirring rate from 400 to 200 rpm decreased the conversion at 2 min by nearly a quarter and at 6 min by half. At the same time, Pd black appeared in the reaction mixture within 1.5 min. It was also found that vials placed farther from the center of the stirring plate experienced better mixing at all stirring rates, due to eccentric motion of the stirring bar, but the conversion varied by a maximum of 10% for different vial positions *under the conditions listed above*. Since most of the kinetic experiments had a much smaller peak oxygen demand, these observations suggested that the reaction rates were at most marginally affected by O_2 dissolution rate.

2.4. Determination of initial rates

The conversion X of benzyl alcohol was calculated from the peak areas of the ^{1}H NMR resonances of benzyl alcohol (δ 4.8 ppm) and benzaldehyde (δ 10.2 ppm), using the formula $X = (2I_{PhCHO})/(2I_{PhCHO} + I_{PhCH2OH})$, where I_x is the peak area for species x. The factor of 2 was due to the different number of protons in those molecules at those resonances. The concentration of benzyl alcohol $C_{BnOH,0}(1 - X)$ decreased with reaction time in a manner that followed approximately first-order kinetics in BnOH for low (<30%) conversions, but which deviated significantly from first-order kinetics at medium and high conversions, primarily due to product inhibition. The available conversion data were fitted with a modified first-order rate law that takes into account product inhibition with an adjustable parameter b (Eq. (1), where $C_{BnOH,0}$ is the initial concentration of BnOH):

$$\frac{d(C_{BnOH})}{dt} = \frac{-kC_{BnOH}{}^2}{C_{BnOH} + b(C_{BnOH,0} - C_{BnOH})} \quad (1)$$

This rate law reduces to first-order kinetics for $t \to 0$ for any value of b (i.e. when no product was present) and also for $b \to 0$. b(=0.30) was obtained by minimizing the average least-squares residual over the entire kinetic data set. The best-fit values of k to experimental data were determined by solving for $C_{BnOH}(t)$ numerically and minimizing the sum of squares of the residuals. Initial rates were then computed with the formula $d(C_{BnOH})/dt|_{t=0} = -kC_{BnOH,0}$. The magnitude of the correction in initial rate obtained with $b = 0.30$ versus $b = 0$ averaged +10%, with a maximum of +26% and a minimum of 0%. While this procedure

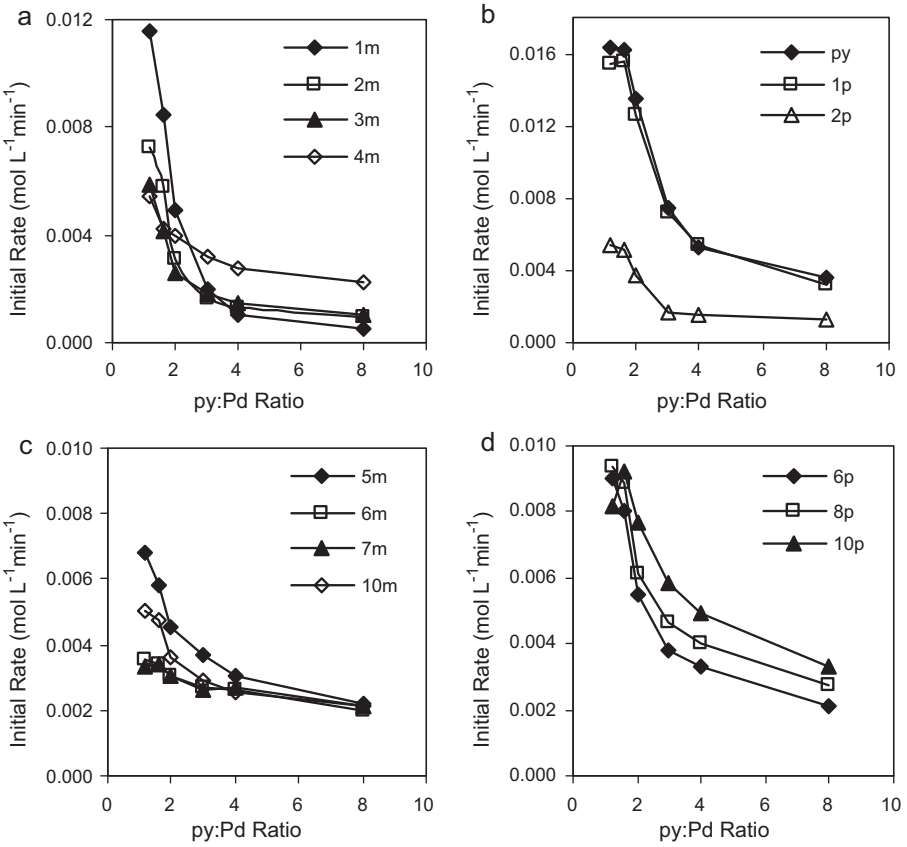

Fig. 1. Effect of ligand (*py* or ^{s}py)-metal ratio on initial rate of BnOH oxidation (353 K, toluene, 5 mM $Pd(OAc)_2$, 20:1 BnOH:Pd). The concentrations of *py* or ^{s}py groups were used to compute the *py*:Pd ratios.

accounted for deactivation due to product inhibition, it did not account for deactivation due to Pd agglomeration. Thus, initial rates estimated by this method would reflect the effect of Pd agglomeration, which typically occurred in the first few minutes of reaction before the first samples were taken. They could be used to compare ligands for their ability to stabilize the Pd complexes.

3. Results

3.1. Effect of ligand–metal ratio on initial rate

The effect of varying the ligand to metal ratio ^{s}py/Pd between 1.2:1 and 8:1 on the initial rate was studied for *py* and the ^{s}py shown in Scheme 1 (reaction conditions: 353 K, 20:1 BnOH:Pd, 5 mM $Pd(OAc)_2$). Fig. 1 shows representative data of initial rates for different ligands. Although for all ligands, increasing the ligand concentration suppressed the activity, the sensitivity of the activity to the ligand concentration depended strongly on the nature of the ligand.

For pyridine, the initial rate decreased by a factor of 4 upon increasing the *py*:Pd ratio by a factor of 4 (from 2:1 to 8:1). Similar, suppression, but of somewhat different magnitudes, was observed for mono(*para*-pyridyl)siloxane **1p** and for bis(*para*-pyridyl)siloxanes **2p**, **6p**, **8p**, and **10p** (Fig. 1b and d). The quantitatively similar activity of **1p** to pyridine suggested that the two ligands are broadly similar in their binding properties. For the tethered ligands, the activity increased with chain length in the order **2p** < **6p** < **8p** < **10p**. A low ^{s}py:Pd ratios, the differences among **6p**, **8p** and **10p** were less significant than at higher ratios.

For mono(*meta*-pyridyl)siloxane **1m**, the activity decreased by a factor of 10 as the ^{s}py:Pd ratio was raised from 1.2:1 to 8:1, much more than for **1p**. For short-chain bis(*meta*-pyridyl)siloxanes **2m** and **3m**, the activity was lower relative to **1m** at ^{s}py:Pd = 1.2, but was slightly higher at ^{s}py:Pd = 8. This trend of weaker dependence of activity on the ^{s}py/Pd ratio continued for medium-chain ligands **4m** and **5m** as well as longer ones. For **6m** and **7m**, the activity decreased by a factor of only 1.5 between ^{s}py:Pd of 1.2:1 and 8:1. The decrease was slightly more pronounced for **10m** over the same ^{s}py:Pd range.

3.2. Effect of ligand on stability of Pd catalysts

The effect of ligand structure on the catalyst stability was investigated under a range of reaction conditions. The variables studied included Pd concentration and BnOH:catalyst ratio. In these experiments, the ^{s}py(or *py*):Pd ratio was fixed at the stoichiometric value of 2 to remove the effect of excess or deficient ligands.

The active site concentration was varied by changing [$Pd(OAc)_2$] while holding the BnOH:catalyst ratio at 20:1. For Pd concentrations of 5 mM (the condition used in Fig. 1) or less, the reaction mixture remained clear throughout the experiment for all ligands studied, suggesting that the catalysts were stable. At the higher Pd concentration of 10 mM, agglomeration of Pd^0 occurred for some ligands (Table 1 and Fig. 2), which was apparent within 2 min of the start of the reaction. At the highest Pd concentration of 20 mM, Pd^0 aggregates were observed for all ligands tested. The data in Table 1 indicated a general trend that the *meta*-pyridylsiloxane ligands were more effective in preventing Pd agglomeration, whereas the *para*-pyridylsiloxanes were similar to or, at best, slightly better than pyridine.

Under conditions used here and when the solution remained clear, i.e. at lower Pd concentrations, the initial reaction rates were

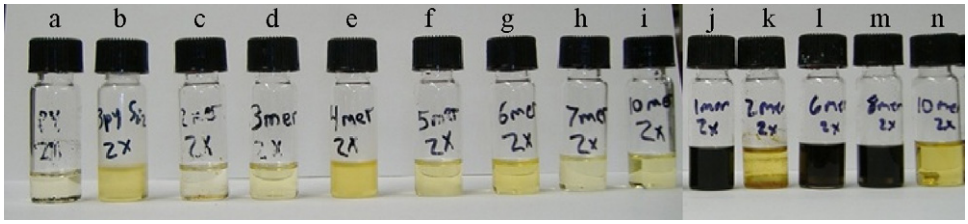

Fig. 2. Appearance of reaction mixture after 10 min of reaction (353 K, toluene, 20:1 BnOH:Pd, 2:^{s}*py*:Pd. 10 mM Pd). Ligand used were: a, *py*; b, **1m**; c, **2m**; d, **3m**; e **4m**; f, **5m**; g, **6m**; h, **7m**; i, **10m**; j, **1p**; k, **2p**; l, **6p**; m, **8p**; n, **10p**. For vial a, black precipitates settled on the bottom.

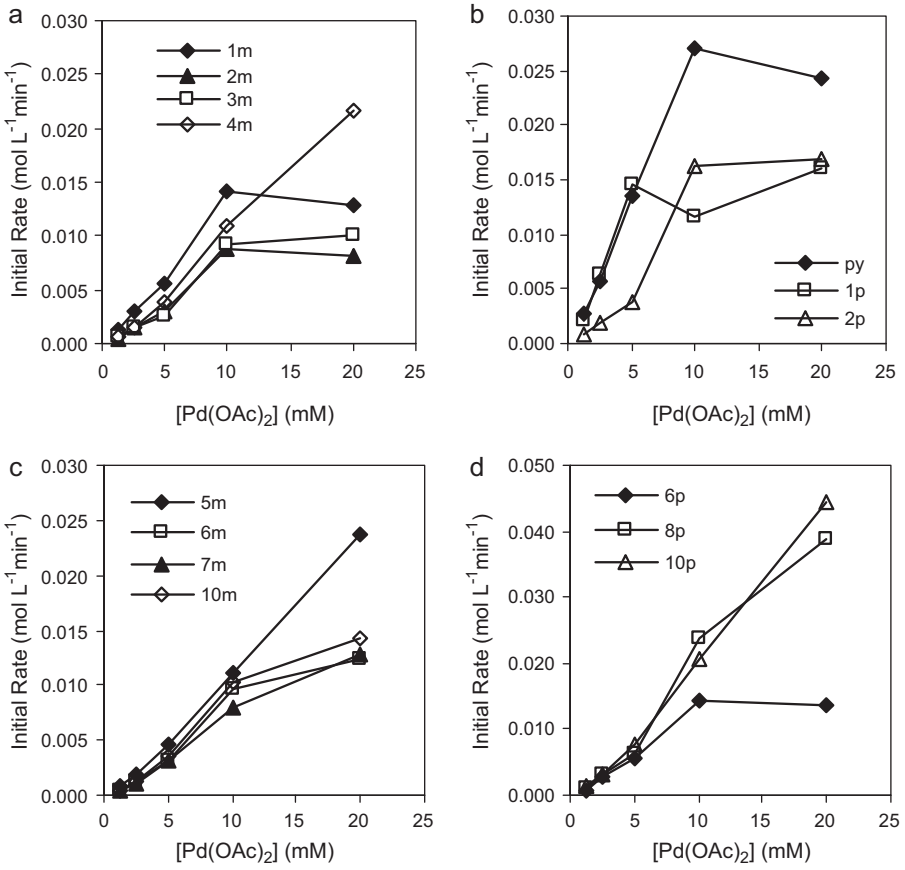

Fig. 3. Dependence of initial reaction rate on Pd concentration (353 K, ^{s}*py*(or *py*)/Pd = 2, BnOH/Pd = 20). Since the ratios of metal, ligand, and substrate were fixed in these experiments, the *x*-axis corresponds to the state of dilution of the reaction system.

expected to show a dependence of $[Pd]^{3/2}$ (see Section 4). This seemed to be the case within experimental uncertainties, which also indicated that the reaction kinetics was not affected by the O_2 dissolution rate at low Pd concentrations (Fig. 3). Except for **4m**, **5m**, and **10p**, the rate was substantially slower at higher Pd concentrations (10 mM or higher) than predicted by the 3/2 order dependence, consistent with loss of catalyst due to formation of less active Pd aggregates. This deviation was particularly noticeable for *py*, **1p**, **2p**, **6p**, **1m**, **2m**, and **3m**.

The long-term stability of the catalysts was also investigated using a reactant concentration of either 25 or 250 mM BnOH and a low Pd concentration of 1.25 mM. This Pd concentration was much lower than those used for Figs. 1 and 2, and was chosen such that there was no detectable formation of Pd black for any of the ligands. Table 2 summarizes the results. All of the ligands tested exhibited good long-term stability, and high turnover numbers were obtained. Thus, at low Pd concentrations, there was no adverse effect with ^{s}*py* ligands. As reported in the literature, buildup of the side product benzoic acid had a negative effect on the activity. As a result, at the higher substrate–catalyst ratio studied, the oxidation activity became strongly suppressed by the side product at long reaction times, such that the reactions were not complete even after 18 h.

4. Discussion

The experimental results show that siloxane-modified pyridine (^{s}*py*) ligands fulfill the mechanistic role of *py* in Pd-catalyzed aerobic oxidation. Broadly speaking, the activities of complexes with ^{s}*py* ligands were within a factor of 3–4 that of *py*, and, as with *py*, they stabilized the Pd complex from agglomeration into Pd black. However, there are significant variations of catalyst activity and stability among the bidentate siloxane ligands with respect to the chain length and the attachment point of silicon to the pyridine ring. These structure–activity trends give further insights into the role of pyridine in the catalytic mechanism, as well as the most important factors affecting the stability of the monomeric Pd active site, particularly at higher Pd concentrations.

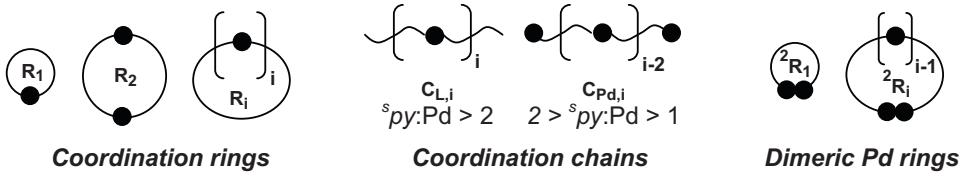

Scheme 2. Schematic representation of some of the various coordination oligomers of $Pd(OAc)_2$ and $^s py$ present in dilute solution. Pd centers are represented as filled dots, and bifunctional ligands as line segments. The complexes denoted by ^2R_i represent rings containing a Pd–Pd bond.

Table 1
Effect of system concentration on catalyst stability (353 K, toluene, 20:1 BnOH:Pd, 2:$^s py$:Pd).

Ligand	[Pd], mM[a]		
	1.25, 2.5, 5[b]	10[b]	20[c]
Pyridine	C	P	B, P
1m	C	C	B
2m	C	C	P
3m	C	C	B
4m	C	C	B, P
5m	C	C	B
6m	C	C	B
7m	C	C	B
10m	C	C	B
1p	C	B	P
2p	C	Y	P
6p	C	B	P
8p	C	B	P
10p	C	Y	P

Reactions were run for 80, 40, 20, 10, and 5 min for Pd concentrations of 1.25, 2.5, 5, 10, and 20 mM, respectively in order to achieve roughly equivalent conversions.
[a] Clear solution (C), intensely yellow but clear solution (Y), black suspension (B), black precipitates (P).
[b] At 400 rpm stirring rate.
[c] At 800 rpm stirring rate.

The data in Fig. 1 show that the activities of all of the *para*-substituted siloxanes, as well as *meta*-pyridylsiloxane **1m** and the short-chain bis(*meta*-pyridyl)siloxanes **2m**, **3m**, and **4m**, were inversely dependent on the total pyridyl concentration in the system, similar to unsubstituted pyridine. In fact, **1p** behaved practically identically to pyridine. However, for longer bis(*meta*-pyridyl)siloxanes **5m** to **10m**, the dependence of activity on [$^s py$] was diminished, with the dependence for **6m** and **7m** being the weakest.

Table 2
Turnover numbers (TONs) at various reaction times using pyridine and ligands **1**–**10** (80 °C, toluene, 2:1 *py*:Pd or $^s py$:Pd, 20:1 or 200:1 BnOH:Pd).

Ligand	TON at sampling time					
	BnOH:Pd = 20[a]			BnOH:Pd = 200[b]		
	24 min	48 min	80 min	60 min	120 min	1080 min
Pyridine	16.5	19.5	20.0	116	132	179
1m	13.8	15.7	18.9	79	102	165
1p	16.3	19.5	20.0	106	128	186
2m	7.0	10.9	15.8	68	93	149
2p	11.8	14.9	14.7	75	100	156
3m	8.6	12.3	14.7	64	87	145
4m	8.6	12.6	15.1	56	73	136
5m	10.2	14.1	15.9	60	75	137
6m	6.5	9.8	13.2	46	59	110
6p	10.3	14.6	15.9	71	92	166
7m	6.9	9.6	11.2	42	54	101
8p	10.3	14.6	18.6	72	89	159
10m	6.5	9.6	10.8	47	60	114
10p	13.9	15.5	17.4	67	85	155

[a] 1.25 mM Pd, 25 mM BnOH.
[b] 1.25 mM Pd, 250 mM BnOH.

Table 3
Experimental effective molarities of cyclic $^s py$–Pd ring complexes R_i (353 K, 5.7 mM in toluene-d_8, 2:$^s py$:Pd), as calculated from ^{1}H NMR measurements of the ring-chain distribution.

Ligand	Effective molarity (EM_i) for R_i (mol L^{-1})			
	EM_1	EM_2	EM_3	EM_4
2m	0	0	0.0030	(0.0063)
3m	0	0.0027	0.0032	(0.0041)
4m	0	0.0075	(0.0063)	(0.0031)
5m	0.0041	0.0091	(0.0046)	(0.0022)
6m	0.0129	(0.0103)	(0.0037)	(0.0018)
7m	0.0162	(0.0086)	(0.0031)	(0.0015)
10m	0.0142	(0.0054)	(0.0019)	(0.0009)
6p	0	0.0071	n.d.	n.d.
8p	0	0.0043	n.d.	n.d.
10p	0.003	0.0058	n.d.	n.d.

The much weaker dependence of activity on $^s py$:Pd ratio for complexes of ligands **5m** to **10m** arise primarily from their ability to form monomeric cyclic coordination complexes R_1 with $Pd(OAc)_2$. Since Pd can normally bind two equivalents of pyridine, and a bis(pyridyl)siloxane can bind two Pd centers, linear and cyclic coordination oligomers can be formed (Scheme 2). The observed ring-chain distribution depends on the ligand structure as well as the concentrations of $^s py$ and $Pd(OAc)_2$ [14–15]. Only R_i are observed for $^s py$/Pd = 2 due to the strong N–Pd bond and the resulting chain termination mechanism from N–Pd bond dissociation. For $^s py$/Pd > 2, linear oligomers $C_{L,i}$ terminated by semibound ligand are formed alongside the ring species, whereas for $^s py$/Pd < 2, $C_{Pd,i}$ terminated by coordinatively unsaturated Pd are formed.

The data in Fig. 1 were collected for $^s py$/Pd = 2. Thus, only ring complexes were expected in these solutions. Among the ring complexes, monomeric R_1 could be formed only if the bidentate ligand is sufficiently long, such that the monomeric ring can be formed with little ring strain. Computational results using the DFT method (B3LYP basis set) suggested that for the bis(*meta*-pyridyl)siloxanes, R_1 formed with **5m** or higher oligomers are essentially strainless, whereas for the *para*-pyridylsiloxanes, oligomers longer than **8p** are required [16]. These computational results were substantiated by experiments. By analyzing the ^{1}H NMR spectra of $^s py$–$Pd(OAc)_2$ at various concentrations and ligand–metal ratios, we found that R_1 was present for bis(*meta*-pyridyl) ligands **5m** and longer and for bis(*para*-pyridyl) ligands longer than **8p** [13]. These results are summarized in Table 3 in terms of effective molarities for R_1 (EM_1). For the R_1 complexes of **5m** to **10m** and **10p**, effective molarities of 3–14 mM were found, which were comparable to the Pd concentrations of 1.25–20 mM used.

Although binding of $^s py$ to Pd is important for stabilizing Pd from deactivation (to be discussed later), Pd complexes of these ligands are less active than Pd–*py* complexes due to ligand competition with BnOH for coordination sites, especially at high $^s py$ concentrations. For these bidentate ligands, because both pyridyl groups are tethered to the siloxane chain, they are never far from the Pd atom even after dissociation from the metal center, since the second pyridyl group is still bound. That is, the effective concentration of the pyridyl groups at the Pd center would be higher

than the average concentration in solution. This effect is expected to be more prominent for shorter ligands that can form R_1. Thus, the activities of **5m** and **6m** are the most suppressed, and they also exhibit the weakest dependence on [^{s}*py*] (Fig. 1). For longer chains, a ^{s}*py* group dissociated from Pd could diffuse farther away, such that the local concentrating effect becomes diluted. Consequently, ligands **8m** and **10p** behave closer to pyridine. For ligands that cannot form R_1, their behavior are like pyridine, as expected.

Steric hindrance also contributes to the suppression of activity. The siloxane tether of a R_1 complex is expected to block access to the Pd center along certain directions. This effect is expected to be more important for R_1 complexes and of shorter ligands for which the siloxane chain is closer to the Pd center, consistent with the observations. Unlike the steric and local concentrating effects, electronic effects due to the siloxane substituents are expected to be negligible. Chvalovsky and coworkers have reported Hammett substituent constants of −0.01 and 0.00 for the *meta*- and *para*-(trimethylsiloxy)dimethylsilyl group, respectively, indicating that the inductive effect of a methylsiloxane substituent on an aromatic ring is negligible [17]. Competitive binding studies conducted by us also showed that **1m** and **1p** bind $Pd(OAc)_2$ with the same affinity as pyridine [13].

The differences in binding properties among the ^{s}*py* ligands correspond to clear trends in the deactivation behavior. Visual observation of the reaction mixtures (Table 1 and Fig. 2) suggested that some ^{s}*py* ligands are more effective in stabilizing Pd from agglomeration than pyridine. In fact, all of the *meta*-pyridylsiloxanes appeared to be superior, in line with the higher effective molarities of pyridyl groups achieved with these ligands. In order to quantify this observation, the apparent initial reaction rates were determined at each of the concentrations shown in Table 1; the results are shown in Fig. 3. In the absence of rapid deactivation, the initial rate is expected to be proportional to $[BnOH][Pd(OAc)_2]^{1/2}$ when the *py*:Pd ratio is 2 [9]. In our experiments, the metal–ligand and substrate–catalyst ratios were unchanged among different ligands; therefore, the initial rate should be proportional to $[Pd]^{3/2}$, where [Pd] is the total Pd concentration. Indeed, at low Pd concentrations (5 mM or less) when no metal agglomeration was detected visually, the expected dependence on [Pd] was observed.

At higher Pd concentrations (10 mM or above), the apparent initial rates dropped off from the expected values due to rapid deactivation of the Pd species, which was essentially complete prior to the time when the first sample was taken. The extent of deviation differed among the ^{s}*py* ligands, and can be used as a qualitative indication of the extent of metal agglomeration. Thus, the *meta*-substituted ligands with a siloxane backbone longer than 3 Si–O units (i.e., **4m** and longer) improve stability of the Pd catalyst from agglomeration, although none of the ligands was able to prevent agglomeration at the high concentration of 20 mM. *Para*-substituted ligands are also effective, but they require longer spacer lengths (8–10 Si–O units). These correlate well with the ability of the ligands to form R_1 complexes – those that can form R_1 complex can stabilize the Pd complex more effectively than those that cannot.

The exception to the above is ligand **4m**. Computational results suggest that a R_1 complex would not be formed with this ligand due to ring strain. We propose that, in this case, a ring complex similar to $^2R_1$ could be formed with this ligand, and the additional Pd atom help relieve the ring strain. Analogous to Pd nanoclusters which have been reported to have some activity in this reaction [18], these $^2R_1$ complexes would also be active for alcohol oxidation, although possibly less than the mononuclear active site. Evidence for Pd–Pd bond formation in similar complexes have been reported by Komano et al. using MALDI mass spectrometry [19].

It should be mentioned that O_2 mass transfer may play a role in these observations. The solubility of O_2 in toluene at 353 K is rather low (ca. 20 mM). Since the initial concentration of substrate is much higher than this, oxygen is consumed most rapidly at the start of the reaction. The drop in O_2 concentration would lead to buildup of Pd^0 species, and eventually Pd black formation. This is expected to be more severe at higher Pd concentrations and with more active catalysts. Therefore, the suppression of activity by the siloxane ligands helps preserve the catalytic activity, in addition to their protective effect by more effective ligation.

5. Conclusion

We have demonstrated that bidentate, bis(pyridyl)siloxane ligands form effective catalysts of Pd complexes. Those ligands that can form monomeric ring complexes result in a catalytic system that exhibits a much weaker dependence of activity on ligand/Pd ratio than those that cannot, and improved catalyst stability. The results demonstrate the importance of effective molarity of ligands on the observed catalytic properties, which are results of steric effect of the siloxane chains, effective local concentration of pyridyl groups, and ability to stabilize Pd^0 complexes against metal agglomeration. The stabilizing effect of bis(pyridyl)siloxane ligands may be useful in catalytic systems where using an excess of pyridine is undesirable or impossible, such as supported Pd complexes. The observations also lead to the possibility of using multi-functional ligands to further tune the catalytic properties by introducing additional and designed interactions between the ligands and the substrate.

Acknowledgements

Support by the U.S. Department of Energy, Basic Energy Sciences, DE-FG02-01ER15184 is gratefully acknowledged. NMR analyses were performed at the IMSERC facility at Northwestern University, using a 400 MHz NMR spectrometer acquired under NSF Grant CHE-9871268 (1998).

Appendix A.

The series of bis(*para*-pyridyl)methylsiloxane ligands was synthesized with materials purchased from either TCI America, Gelest, or Sigma-Aldrich, which were used as received. Manipulations of air- and moisture-sensitive chemicals were performed using a Schlenk line under N_2. Spectroscopic and HRMS data were collected in the IMSERC facility at Northwestern University. NMR spectra were collected on a Varian INOVA 400 MHz spectrometer with a broadband probe.

4-Pyridyldimethylsilane (1a): 5.00 g of 4-bromopyridine hydrochloride (TCI America, 0.0257 mol) was weighed into a 250 mL Erlenmeyer flask, and a magnetic stir bar was added. Approximately 125 mL of a 5% aqueous solution of Na_3CO_3 were added and stirred until the product dissolved, bubbling stopped, and the pH was greater than 8.5 (<5 min). The reaction mixture was washed with 2× 50 mL portions of water and 1× 50 mL brine. The organic phase was dried with $MgSO_4$, and solvents were removed by rotary evaporation to obtain the free base (3.3 g yield, 0.021 mol). The free base was injected into a 100 mL Schlenk flask containing 25 mL of anhydrous THF, and equipped with a magnetic stir bar and rubber septum under N_2. To this solution, 12 mL of a 2.0 M solution of isopropylmagnesium chloride in THF were added by syringe over 1 min, causing the reaction mixture to turn orange. The reaction was allowed to proceed for 1.5 h at room temperature. Finally, 2.8 mL (0.025 mol) of chlorodimethylsilane was added slowly. The reaction mixture warmed and the orange color slowly

discharged. Reaction was allowed to proceed for 1 h. The reaction mixture was diluted in 2 parts of diethyl ether, washed with 2× 50 mL portions of distillated water and 1× 50 mL of brine, and dried over Na_2SO_4. Solvents were removed by rotary evaporation to yield a free-flowing yellow oil in good yield (2.6 g, 0.019 mol, 91% from free base). Further purification was accomplished by vacuum distillation (20 Torr, 75 °C) to give 1.95 g of **1a** as a clear colorless liquid (0.014 mol, 75%). ^{1}H NMR (400 MHz, $CDCl_3$): δ 8.54 (d, J_{AB} = 4.4 Hz, 2H), 7.38 (dd, J_{BA} = 4.2, $J_{BB'}$ = 1.4 Hz, 2H), 4.38 (sept, J_D = 3.8 Hz, 1H), 0.34 (J_C = 3.8 Hz, 6H) ppm. ^{13}C NMR (100 MHz, $CDCl_3$): δ 149.02, 148.88, 129.04, −4.45 ppm. ^{29}Si NMR (80 MHz, $CDCl_3$): δ −19.8 ppm. HRMS (ESI) calcd for $C_7H_{11}NSi$ ([M + H]$^+$): *m*/*z* 138.0734; found 138.0733.

4-Pyridyldimethylsilanol (1b): A 50 mL Schlenk flask equipped with magnetic stir bar and rubber septum was connected to an oil bubbler and purged with a stream of N_2, then charged with 20 mg of Pearlman's catalyst (20 wt% $Pd(OH)_2$/C), 19 mL of tetrahydrofuran, and 1 mL of water. The reaction was stirred while 1.0 g (6.5 mmol) of **1a** was added by syringe. Evolution of H_2, as monitored with bubbler, was complete within 4 hours. The reaction was then syringe-filtered to remove the catalyst and evacuated (final pressure ca. 50 mTorr) to remove solvents and water. The product **2p** was isolated as a turbid oil (when impure) or in crystalline form. Isolated yields of greater than 90% were achieved with less than 10% being the homofunctional condensation product bis(4-pyridyl)-tetramethyldisiloxane. Product was found to be marginally stable in the pure state at room temperature, with a half-life of greater than 24 h. ^{1}H NMR (400 MHz, $CDCl_3$): δ 8.41 (dd, J_{AB} = 4.2 Hz, $J_{AA'}$ = 1.5 Hz, 2H), 7.46 (dd, J_{BA} = 4.3 Hz, $J_{BB'}$ = 1.5 Hz, 2H), 6.40 (bs, 1H), 0.38 (s, 6H) ppm. ^{13}C NMR (100 MHz, $CDCl_3$): δ 151.10, 148.12, 128.41, 0.08 ppm. ^{29}Si NMR (80 MHz, $CDCl_3$): δ 3.74 ppm. HRMS (ESI) calcd for $C_7H_{11}NOSi$ ([M + H]$^+$): *m*/*z* 154.0683; found 154.0674.

1-(4-Pyridyl)-1,1,3,3-tetramethydisiloxane (1c): Prepared in the same manner as **1b**, but rather than isolating the product, the silanol (6.9 mmol) was redissolved with anhydrous diethyl ether in a 50 mL Schlenk flask which was previously connected to an oil bubbler and purged with N_2. Into this flask was injected 2.15 mL (15.4 mmol) of triethylamine, followed immediately by 1.55 mL (14 mmol) of chlorodimethylsilane. The reaction mixture turned into a voluminous white precipitate accompanied by a significant amount of fuming. The reaction mixture was washed with 2× 50 mL portions of water, followed by 1× 30 mL of brine, and volatile components were removed by rotary evaporation to give 1.23 g of **1c** as a clear liquid (5.4 mmol, 78%). ^{1}H NMR (400 MHz, $CDCl_3$): δ 8.57 (dd, J_{AB} = 4.4 Hz, $J_{AA'}$ = 1.2 Hz, 2H), 7.40 (dd, J_{BA} = 4.3 Hz, $J_{BB'}$ = 1.3 Hz, 2H), 4.75, (sept, J = 2.8 Hz, 1H), 0.35 (s, 6H), 0.19 (d, J = 2.8 Hz, 6H) ppm. ^{13}C NMR (100 MHz, $CDCl_3$): δ 147.0, 146.4, 125.5, −1.44, −2.07 ppm. ^{29}Si NMR (80 MHz, $CDCl_3$) δ −0.82, −3.86 ppm. HRMS (ESI) calcd for $C_9H_{18}NOSi_2$ ([M + H]$^+$): *m*/*z* 212.0921; found 212.0920.

1-(4-Pyridyl)-1,1,3,3-tetramethyldisiloxanol (1d): Prepared in the same manner as **1b** from 1.23 g (5.4 mmol) of **1c**. Evolution of H_2 was complete within 4 h. The product **1d** was isolated as 1.1 g (4.9 mmol, 91%) of a colorless oil. ^{1}H NMR (400 MHz, $CDCl_3$): δ 8.41 (dd, J_{AB} = 4.3 Hz, $J_{AA'}$ = 1.4 Hz, 2H), 7.40 (dd, J_{BA} = 4.3 Hz, $J_{BB'}$ = 1.5 Hz, 2H), 5.58 (bs, 1H), 0.36 (s, 6H), 0.14 (s, 6H) ppm. ^{13}C NMR (100 MHz, $CDCl_3$): δ 150.2, 148.0, 128.0, 0.63, 0.39 ppm. ^{29}Si NMR (80 MHz, $CDCl_3$) δ −2.82, −10.40 ppm. HRMS (ESI) calcd for $C_9H_{17}NO_2Si_2$ ([M + H]$^+$): *m*/*z* 228.0871; found 228.0870.

1-(4-Pyridyl)-1,1,3,3,5,5-hexamethyltrisiloxane (1e): Prepared in the same manner as **1c**, from 6.9 mmol of **1d**. After washing and removal of solvents 0.55 g of **1e** was obtained (1.9 mmol, 83%). ^{1}H NMR (400 MHz, $CDCl_3$): δ 8.57 (dd, J_{AB} = 4.3 Hz, $J_{AA'}$ = 1.2 Hz, 2H), 7.41 (dd, J_{BA} = 4.2 Hz, $J_{BB'}$ = 1.2 Hz, 2H), 4.68 (sept, J_{CD} = 2.8 Hz, 1H), 0.35 (s, 6H), 0.15 (d, J = 2.8 Hz, 6H), 0.07 (s, 6H) ppm. ^{13}C NMR (100 MHz, $CDCl_3$): δ 149.4, 148.8, 127.8, 0.74, 0.41 ppm. ^{29}Si NMR (80 MHz, $CDCl_3$): δ −3.2, −6.6, −18.0 ppm. HRMS (ESI) calcd for ([M + H]$^+$): *m*/*z* 286.1111; found 286.1109.

1-(4-Pyridyl)-1,1,3,3,5,5-hexamethyltrisiloxan-3-ol (1f): Prepared in the same manner as **1d**, from 1.23 g (5.4 mmol) of **1e**. Evolution of H_2 was complete within 4 h. The product **1f** was isolated as 1.1 g (4.9 mmol, 91%) a turbid oil. ^{1}H NMR (400 MHz, $CDCl_3$): δ 8.49 (dd, J_{AB} = 4.3 Hz, $J_{AA'}$ = 1.1 Hz, 2H), 7.42 (dd, J_{BA} = 4.4 Hz, $J_{BB'}$ = 1.3 Hz, 2H), 5.32 (bs, 1H), 0.34 (s, 6H), 0.10 (s, 6H), 0.08 (s, 6H). ^{13}C NMR (100 MHz, $CDCl_3$): δ 150.81, 148.15, 127.98, 1.25, 0.52, 0.41 ppm. ^{29}Si NMR (80 MHz, $CDCl_3$) δ −3.35, −12.64, −19.74 ppm. HRMS (ESI) calcd for $C_7H_{11}NOSi$ ([M + H]$^+$): *m*/*z* 302.1058; found 302.1059.

(**4-Pyridyl)pentamethyldisiloxane (1p)**: Prepared according to the synthesis of **1b** on the 0.139 g (0.91 mmol) scale, except that chlorotrimethylsilane (2 mmol) is used in the condensation step. Purified by column chromatography. Yield 0.151 g (1.14 mmol, 74% from **1b**). ^{1}H NMR (400 MHz, $CDCl_3$): δ 8.57 (dd, J = 4.3 Hz, 1.1 Hz, 2H), 7.38 (dd, J = 4.3 Hz, 1.1 Hz, 2H), 0.32 (s, 6H), 0.09 (s, 9H) ppm. ^{13}C NMR (100 MHz, $CDCl_3$): δ 149.7, 148.9, 127.8, 2.04, 0.61 ppm. ^{29}Si NMR (80 MHz, $CDCl_3$): δ 6.11, −7.21 ppm. HRMS (ESI) calcd for $C_{10}H_{19}NOSi_2$ ([M + H]$^+$): *m*/*z* 226.1078; found 226.1083.

1,3-Bis(4-pyridyl)tetramethyldisiloxane (2p): Prepared according to the synthesis of **1c**, except that 1.0 g (6.5 mmol) of 4-pyridyldimethylsilanol (**1b**) was isolated and warmed to 100 °C under vacuum for 2 h. Purified by column chromatography on silica gel. Yield 0.27 g (0.94 mmol, 29%). ^{1}H NMR (400 MHz, $CDCl_3$): δ 8.58 (dd, J_{AB} = 4.1 Hz, $J_{AA'}$ = 1.1 Hz, 2H), 7.37 (dd, J_{BA} = 3.9 Hz, $J_{BB'}$ = 1.2 Hz, 2H), 0.36 (s, 12H) ppm. ^{13}C NMR (100 MHz, $CDCl_3$): δ 153.7, 150.7, 140.8, 134.2, 123.5, 0.96 ppm. ^{29}Si NMR (80 MHz, $CDCl_3$): −0.1 ppm. HRMS (ESI) calcd for $C_{14}H_{20}N_2Si_2O$ ([M + H]$^+$): *m*/*z* 289.1187; found 289.1191.

1,11-Bis(4-pyridyl)dodecamethylhexasiloxane (6p): Prepared from 1.0 g (6.5 mmol) of **1b** and 1.16 g (3.3 mmol) 1,7-dichlorotoctamethyltetrasiloxane. Purified by chromatography on silica gel. Yield 0.66 g (1.1 mmol, 51%). ^{1}H NMR (400 MHz, $CDCl_3$): δ 8.59 (dd, J_{AB} = 4.2 Hz, $J_{AA'}$ = 1.4 Hz, 2H), 7.42 (dd, J_{BA} = 4.2 Hz, $J_{BB'}$ = 1.5 Hz, 2H), 0.36 (s, 12H), 0.09 (s, 12H), 0.05 (s, 12H). ^{13}C NMR (100 MHz, $CDCl_3$): δ 148.9, 137.7, 127.8, 1.3, 1.2, 0.46 ppm. ^{29}Si NMR (80 MHz, $CDCl_3$): δ −7.1, −23.8, −25.6 ppm. HRMS (ESI) calcd. for $C_{22}H_{44}N_2O_5Si_6$ ([M + H]$^+$): *m*/*z* 585.1939; found 585.1929.

1,15-Bis(4-pyridyl)hexadecamethyloctasiloxane (8p): Prepared from 1.0 g (4.4 mmol) of **1d** and 0.77 g (2.2 mmol) 1,7-dichlorotoctamethyltetrasiloxane. Purified by chromatography on silica gel. Yield 0.77 g (1.1 mmol, 48%). ^{1}H NMR (400 MHz, $CDCl_3$): δ 8.58 (dd, J_{AB} = 4.3 Hz, $J_{AA'}$ = 1.2 Hz, 2H), 7.41 (dd, J_{BA} = 4.2 Hz, $J_{BB'}$ = 1.4 Hz), 0.35 (s, 12H), 0.09 (s, 12H), 0.06 (s, 12H), 0.05 (s, 12H). ^{13}C NMR (100 MHz, $CDCl_3$): δ 149.4, 148.8, 127.8, 1.2, 1.1, 0.43 ppm. ^{29}Si NMR (80 MHz, $CDCl_3$): δ −2.8, −19.5, −21.3, −21.4 ppm. HRMS (ESI) calcd. for $C_{26}H_{56}N_2O_7Si_8$ ([M + H]$^+$): *m*/*z* 733.2314; found 733.2305.

1,19-Bis(4-pyridyl)icosamethyldecasiloxane (10p): Prepared from 1.0 g (3.3 mmol) of **1f** and 0.58 g (1.7 mmol) 1,7-dichlorotoctamethyltetrasiloxane. Purified by chromatography on silica gel. Yield 0.64 g (1.1 mmol, 44%). ^{1}H NMR (400 MHz, $CDCl_3$): δ 8.59 (dd, J_{AB} = 4.2 Hz, $J_{AA'}$ = 1.4 Hz, 2H), 7.42 (dd, J_{BA} = 4.2 Hz, $J_{BB'}$ = 1.5 Hz, 2H), 0.36 (s, 12H), 0.09 (s, 12H), 0.05 (s, 12H). ^{13}C NMR (100 MHz, $CDCl_3$): δ 149.5, 148.9, 1.2, 0.5 ppm. ^{29}Si NMR (80 MHz, $CDCl_3$): δ −2.7, −19.4, −21.2, −21.4 ppm. HRMS (ESI) calcd. for $C_{30}H_{68}N_2O_9Si_{10}$ ([M + H]$^+$): *m*/*z* 881.2690; found 881.2698.

References

[1] S.S. Stahl, Science 309 (2005) 1824–1826.

[2] T. Nishimura, T. Onoue, K. Ohe, S. Uemura, Tetrahedron Letters 39 (1998) 6011–6014.
[3] M.S. Sigman, D.R. Jensen, Accounts of Chemical Research 39 (2006) 221–229.
[4] J.H. Liu, F. Wang, X.L. Xu, Progress in Chemistry 19 (2007) 1718–1726.
[5] T. Nishimura, S. Uemura, Synlett (2004) 201–216.
[6] D.R. Jensen, J.S. Pugsley, M.S. Sigman, Journal of the American Chemical Society 123 (2001) 7475–7476.
[7] J.A. Mueller, D.R. Jensen, M.S. Sigman, Journal of the American Chemical Society 124 (2002) 8202–8203.
[8] S.K. Mandal, D.R. Jensen, J.S. Pugsley, M.S. Sigman, Journal of Organic Chemistry 68 (2003) 4600–4603.
[9] B.A. Steinhoff, I.A. Guzei, S.S. Stahl, Journal of the American Chemical Society 126 (2004) 11268–11278.
[10] B.A. Steinhoff, S.S. Stahl, Organic Letters 4 (2002) 4179–4181.
[11] B.V. Popp, S.S. Stahl, Chemistry-A European Journal 15 (2009) 2915–2922.
[12] Ta. Stephens, Sm. Morehous, A.R Powell, J.P. Heffer, G. Wilkinso, Journal of the Chemical Society (1965) 3632.
[13] M.N. Missaghi, J.N. Galloway, H.H. Kung, Organometallics 29 (2010) 3769–3779.
[14] H. Jacobson, W.H. Stockmayer, Journal of the Chemistry and Physics 18 (1950) 1600–1606.
[15] G. Ercolani, L. Mandolini, P. Mencarelli, S. Roelens, Journal of the American Chemical Society 115 (1993) 3901–3908.
[16] I. Konstantinov, J.M. Galloway, M.N. Missaghi, L.J. Broadbelt, H.H. Kung, Journal of Physical Chemistry C (submitted for publication).
[17] Z. Plzak, F. Mares, J. Hetflejs, J. Schraml, Z. Papouskova, V. Bazant, E.G. Rochow, V. Chvalovsky, Collection of Czechoslovak Chemical Communications 36 (1971) 3115–3127.
[18] K. Wada, K. Yano, T. Kondo, T.A. Mitsudo, Catalysis Letters 112 (2006) 63–67.
[19] T. Komano, T. Iwasawa, M. Tokunaga, Y. Obora, Y. Tsuji, Organic Letters 7 (2005) 4677–4679.